JOURNAL OF MATERIALS SCIENCE 28 (1993) 3043–3048

Fibrillar structure of superdrawn polyoxymethylene fibres

T. KOMATSU
Analytical Research Centre of Asahi Chemical Industry Co. Ltd, 2-1 Samejima, Fuji, Sizuoka 416, Japan

A fibre structure of superdrawn polyoxymethylene fibres was examined by scanning electron microscopy. The fibre had a skin–core structure and was characterized by a double fibrillar network which was formed from a frame network of trunk fibril screens parallel to the fibre axis, a sub-network of branch fibrils inside the frame, thin cross-fibrils connected to the network and longitudinal void-chains connected to the cross-fibrils between the fibril screens. The frame fibrillar network originated in the undrawn spherulite network, trunk and branch fibrils originated in a bundle of lamellar crystallites and cross-fibrils probably resulted from the interlamellar amorphous phase. The fibrillar network was also varied in the radius direction, possibly due to the diversities of the undrawn spherulitic morphology and the deformation mode at necking.

1. Introduction

Fibrillar structures of highly oriented polymer fibres, which are responsible for an enhancement of mechanical properties such as Young's modulus and tensile strength, have been extensively studied from morphological and mechanical viewpoints [1–15]. The structure varies with degrees of drawing: in the region of natural to moderate draw ratios, the structure is transformed into a stacking structure of lamellar crystallites and amorphous phase oriented to the drawing direction from a random spherulitic structure before drawing [1–9]; at ultra-high draw ratios, a completely oriented fibrillar structure is formed for an ultra-high molecular weight polyethylene (UHMWPE) [15, 16]. The structure also differs depending on processing and polymer species: perfectly extended molecular chains for needle-like polyoxymethylene (POM) crystals polymerized from a dilute trioxane solution [17], a skin–core structure of oriented microfibrils for a Kevlar fibre [18], a highly chain-extended structure for ultra-drawn polyoxymethylene fibres [14, 19], perfectly oriented smooth fibrils via shish-kebab structure for gel-spun/hot-drawn UHMWPE fibres [13, 20], and highly oriented fibrils including lateral lamellae for zone-drawn UHMWPE fibres [21].

These fibres usually have an extremely high tensile modulus, sometimes very close to the theoretical values, as obtained for polyethylene [16, 17] and isotactic polypropylene [22–25]. The experimental modulus may be determined from the initial slope of a stress–strain curve in the elastic deformation region (usually within 0.1% strain) and relates to the microstructure parameters in the region of a few to several tens of nanometres in dimension, i.e. orientation factor, crystallinity, crystallite size. Therefore, the tensile modulus can be estimated using an adequate mechanical model of fibrillar structure. The experimental Young's modulus of ultradrawn polyoxymethylene and polyethylene fibres have been shown to be well explained by Takayanagi's model or the modified model [11, 26, 27].

However, tensile strength is almost impossible to predict using any mechanical model. This mainly arises for two reasons: (1) the strength is a result of fracture occurring in the region of plastic deformation; (2) the molecular weight of real fibres is much too small to be compared with the sample length between the clamps. In other words, the difficulty in evaluating the strength is due to the fracture process of real fibres being governed by various defects included in the samples. The mechanical models are much simplified in order to perform a theoretical calculation and they ignore the effect of defects on strength.

Analysis of real fibrillar structures including defects is therefore a base requirement for the understanding of tensile strength, and will be also effective in clarifying fracture process, plastic deformation and stress relaxation. In the present work, as the starting point for understanding these fundamental properties, the fibrillar structure of superdrawn polyoxymethylene fibres was studied in detail by scanning electron microscopy and is discussed with respect to an undrawn spherulitic structure.

2. Experimental procedure

2.1. Sample preparation

A tube of outer diameter 1.5 mm and inner diameter 0.5 mm was prepared by melt extrusion of an acetal homopolymer (Tenac 3010, Asahi Chemical Industry

0022–2461

Co. Ltd) at 195 °C, followed by quenching in cold water at 10 °C. The tube was continuously two-step drawn in high-pressure silicone oil according to the method given previously [28]. The drawing conditions were as follows: in the first step, vessel length 12 m, feed speed 0.5 m min^{-1}, draw ratio 8, drawing temperature 150 °C and gauge pressure 50 kg cm^{-2}; in the second step, vessel length 45 m, total draw ratio 30, drawing temperature 170 °C and gauge pressure 200 kg cm^{-2}. The resultant fibre was washed with freon-113 to remove completely any silicone oil adhering to the fibre, and it was then vacuum dried at 100 °C for 2 h.

2.2. Sample preparation for SEM observation

The longitudinal section of the fibre was prepared as follows: the fibre of ~50 mm length was embedded in an epoxy resin (Ciba-Geigy Co., "Araldite rapid"), cut into pieces ~2 mm long, mounted on a specimen support, trimmed parallel to the fibre axis at the fibre diameter by a razor-microtome and smoothed using a glass knife. The cross-section of the fibre was prepared by embedding in an epoxy resin (Oukenn Syouji Co., "EPOC 812") under the conditions given previously [29]. The cross-section of the embedded fibre was then trimmed with a razor, smoothed with a glass knife and finished with a diamond knife. The cured epoxy resin in the cross-section was removed using dimethylsulphoxide (DMSO) at 90 °C for 1 h, followed by extraction of DMSO with acetone and vacuum drying at room temperature.

2.3. Observation of spherulitic morphology of the undrawn tube

The spherulitic morphology of the undrawn tube was observed using a polarizing microscope and a thin cross-sectional film of ~20 μm thickness prepared using a microtome. The chemically etched cross-section of the undrawn tube was also observed by SEM. Etching was carried out in an aqueous 2% solution of phosphotungstic acid at 90 °C for 4 h.

2.4. SEM observation

The samples were lightly gold coated and examined by scanning electron microscopy (Hitachi Seisakusyo Co., S-430 operated at 5 kV).

3. Results

3.1. Fibrillar structure

Fig. 1 shows a micrograph of the surface of a white fibre (draw ratio 30, Young's modulus 59.5 GPa, tensile strength 1.9 GPa and void volume fraction 32%). Voids were rarely observed in the surface despite a high quantity of voids present in the sample. Hence, the inside of the fibre was examined. Fig. 2 shows a scanning electron micrograph of a longitudinal section of the same fibre. Fibrils parallel to the fibre axis, cross-fibrils connected in a ladder-like

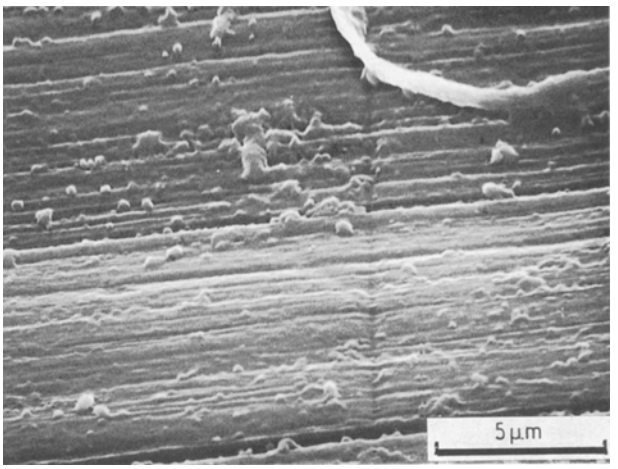

Figure 1 Scanning electron micrograph of the surface of a superdrawn POM fibre, showing a smooth surface.

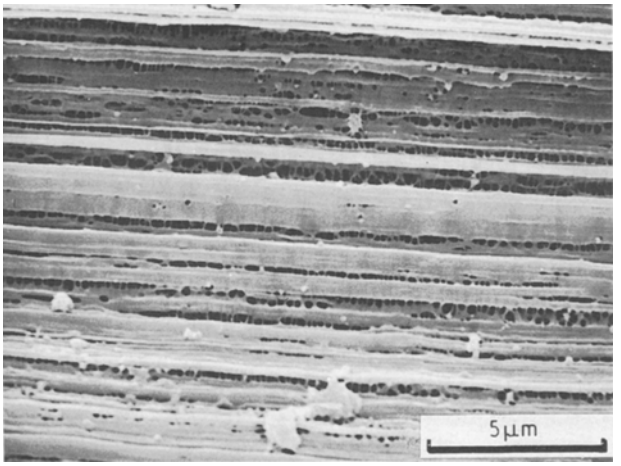

Figure 2 Scanning electron micrograph of the longitudinal section of a superdrawn POM fibre, showing a fibrillar structure including voids.

manner to the neighbouring fibrils, and microvoids between the fibrils which separated from each other by cross-fibrils, are clearly observed. This structure is similar to that of an elemental microfibril of an ultra-drawn UHMWPE film which consists of a parallel fibril of 0.04 μm and lateral fibril of 0.01 μm thick [16]. For the present polyoxymethylene fibre, the dimensions of these components were ~1 μm thick for parallel thick fibrils and ~0.05 μm thick for cross-fibrils.

A scanning electron micrograph of the cross-section of the same fibre also gave more detailed information on fibrillar structure. The fibre had a complex fibrillar network, as shown in Fig. 3a. The fibrillar network is characterized by its organization and morphology: the structure consists of frame networks of two trunk fibrils of different thickness, one about 1 μm and the other about 0.2 μm thick (Fig. 3b), sub-networks of branch fibrils about 0.3 μm thick branching inside the cell unit of the frame, cross-fibrils about 0.05 μm thick connecting to branch fibrils and voids between the fibrils (Fig. 3c; where the flat material found in some places is the remaining epoxy resin); morphologically,

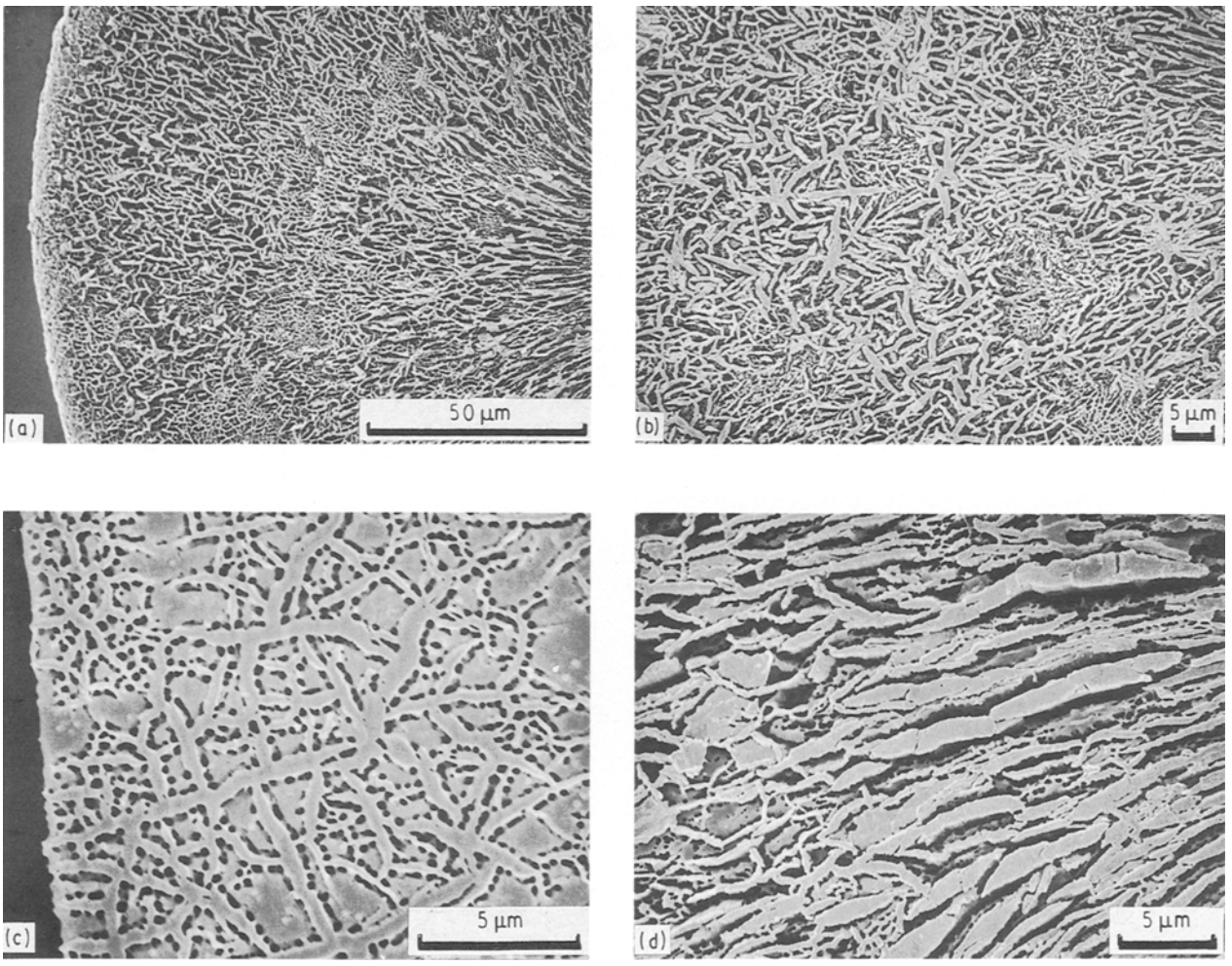

Figure 3 Scanning electron micrographs of the cross-section of a superdrawn POM fibre: (a) one side of the cross-section showing a complex fibrillar network; (b) observation at the half-radius which shows radial networks of thick fibrils and networks of thin fibrils; (c) slender fibrils radially extending from the fibre centre; (d) microstructure revealing a double-frame network consisting of frame networks of trunk fibrils, sub-networks of branch fibrils inside the frame cell, cross-fibrils connected to fibrils, and voids between fibrils.

lattice networks are found near the surface (Fig. 3a), radial networks at the half radius (Fig. 3b) and networks of slender fibrils radially extending towards the fibre centre (Fig. 3d). Fig. 3a also shows that the fibre has a skin–core structure, being very dense at the uppermost surface but porous at a more interior point. Due to this dense skin layer, voids were rarely observed in the intact sample surface, as was found for superdrawn polyoxymethylene fibres prepared under high pressure [29].

3.2. Characterization of fibrillar network

As shown in Fig. 3a, the shape of the frame network was heterogeneous and drastically varied in the radius direction of the fibre. The sizes of trunk fibrils and voids were measured from scanning electron micrographs. The fibril length in the cross-section was taken as the distance along its length and the fibril thickness was taken at the centre of the length. The size parameters (length, thickness), of fibrils were measured at the half-radius and fibre center, because the morphologies at each position were relatively homogeneous. These parameters were, respectively, approximately 8 and 1 μm, at the half-radius from Fig. 3b, and approximately (15 and 1.5 μm) at the fibre centre from Fig. 3d. The length of cross-fibrils along the voids was taken as the void diameter. The distribution of voids was obtained by image analysis used in previous work [29]. Voids had a narrow distribution showing a diameter of ~ 0.2 μm at the peak.

3.3. Undrawn spherulitic morphology preceding fibrillar structure

The complex fibrillar structure of superdrawn polyoxymethylene fibres is naturally supposed to be related to the undrawn spherulitic morphology and its deformation process during drawing. Fig. 4a–c show scanning electron micrographs of a chemically etched cross-section of the undrawn tube, indicating spherulites which consist of lamellar crystallites selectively left after chemical removal of the amorphous phase. This indicates spherulite diameters to be heterogeneous in the radial direction: small spherulites of ~ 5 μm were generated at the outer surface (Fig. 4a), growing to larger spherulites of ~ 25 μm at the half-radius (Fig. 4b) and very large spherulites of ~ 50 μm at the tube centre (Fig. 4c).

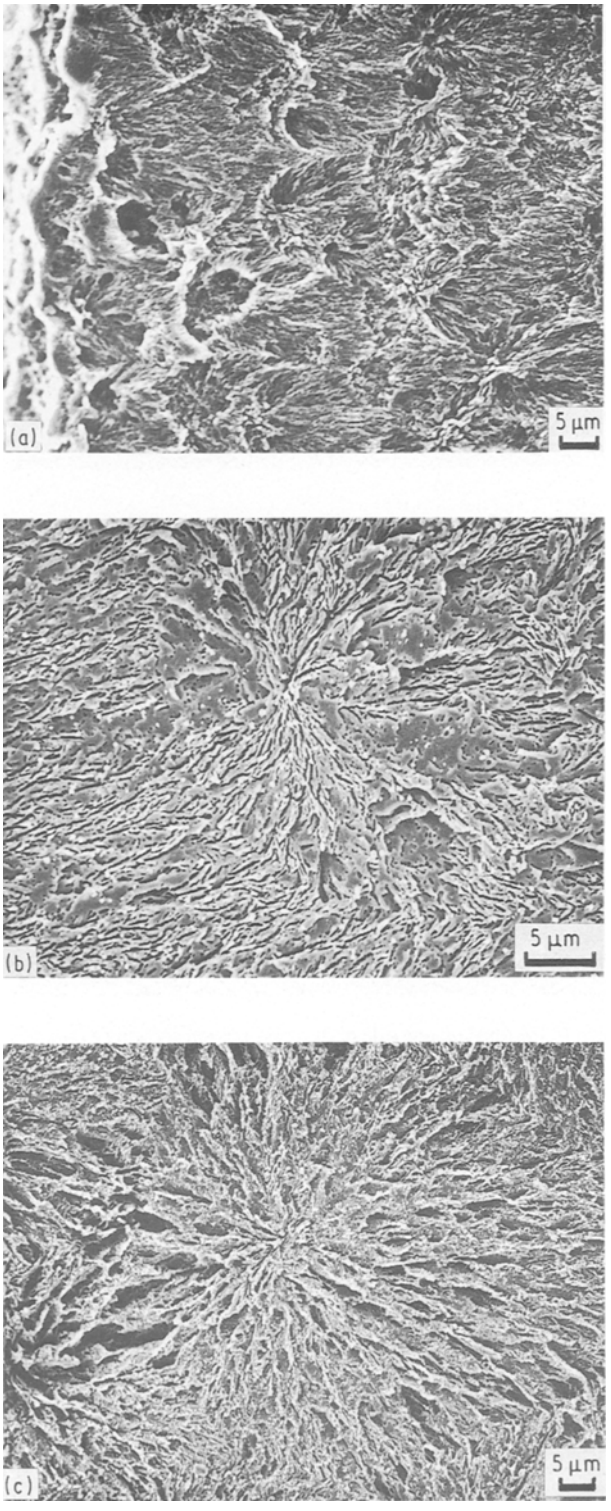

Figure 4 Scanning electron micrographs of the chemically etched cross-section of undrawn POM tube: (a) small spherulites in the outer surface; (b) larger spherulites observed at the half-radius; (c) large spherulites observed at the tube centre.

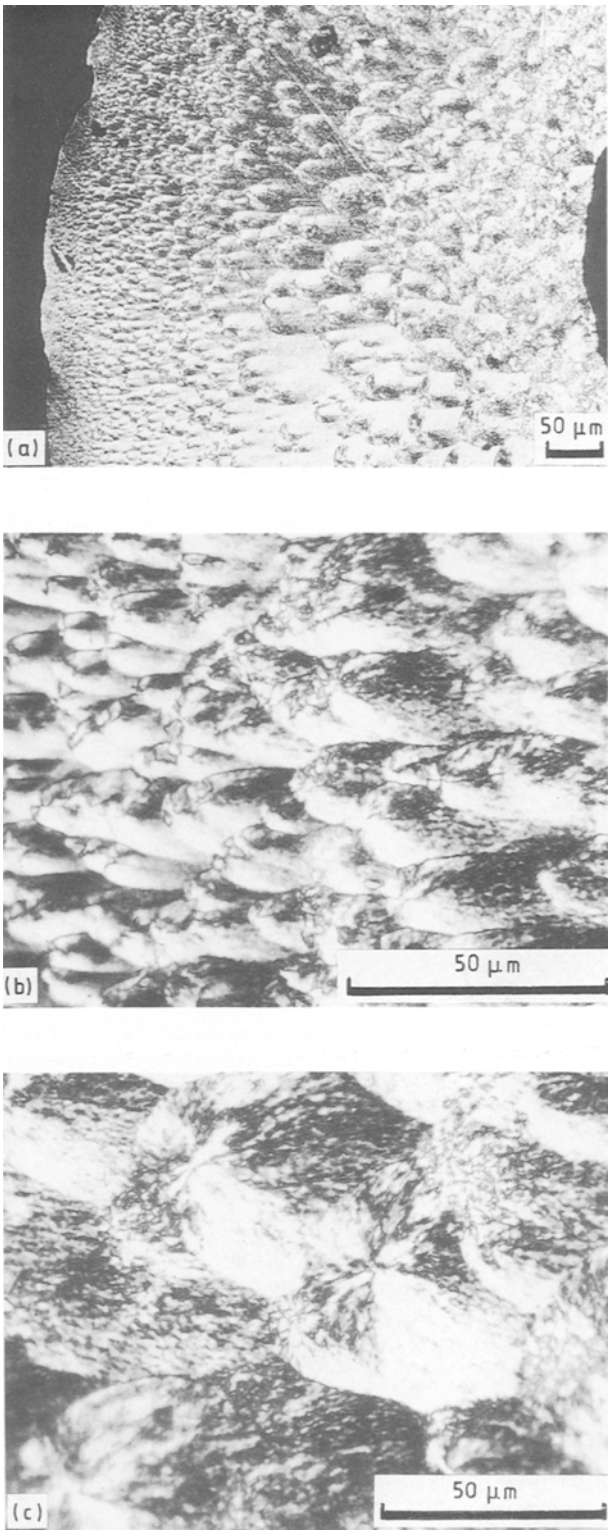

Figure 5 Polarizing micrographs of the cross-section of an undrawn POM tube: (a) one side of the cross-section showing different spherulitic morphologies in the radius direction; (b) ellipsoid spherulites at the half-radius growing towards the tube centre; (c) large square spherulites at the tube centre.

Fig. 5a–c show polarizing micrographs of a cross-section of the same tube, indicating the same heterogeneities in the size and morphology of spherulites as those in Fig. 4. This heterogeneous structure is clearly due to the cooling process after extrusion in which a molten resin was quenched to the solid tube: at the surface in contact with the cold medium, small crystallites were formed by rapid cooling; at more inner points, larger spindle-shaped spherulites were generated owing to slower crystallization under slow cooling; the shape is due to the growth crystallites towards the centre direction according to a temperature gradient; at the tube centre, very large square spherulites were formed by adiabatic cooling.

4. Discussion

4.1. Origin of fibrillar structure

The variety of sizes of fibrillar networks in the radius

direction as shown in Fig. 3a is clearly related to change in spherulite sizes in Fig. 4: small fibrillar networks at the surface and relatively larger networks in the inside correspond to small crystallites and larger spherulites, respectively, except for the peculiar morphology of networks extending radially from the fibre centre. Assuming spherulites to be stretched along the fibre axis, the cross-sectional area of fibrils, S, is related to the draw ratio, λ ($=30$), and the spherulite mean diameter, D (the mean value of long and short diameters of ellipsoidal spherulites was used to simplify the calculation) by the following equation [15]

$$\lambda = (\pi D^2/4)S^{-1} \quad (1)$$

In the case of radial fibrils similar to the spherulitic shape, S is given as $\pi d^2/4$, where d is the fibril thickness. The observed values were D $\simeq 25$ μm and $d \simeq 4.5$ μm from Figs 3b and 4b, satisfying the equation quite well. In the case of slender radial fibrils, S is given as TL, where T and L are the distance between neighbouring fibrils and the fibril length in the cross-section, respectively. The observed values were $D \simeq 50$ μm, $T \simeq 4.5$ μm and $L \simeq 15$ μm from Figs 3d and 4c. The values again satisfy the equation quite well.

These values indicate the unit of a thick-frame network to originate in the spherulites. In the same way, the unit of a thin-frame network emanates from small crystallites in the region surrounded by spherulites, as shown in Fig. 4b. Each trunk and branch fibril naturally results from a bundle of lamellar crystallites constituting the spherulites. Cross-fibrils probably result from interlamellar amorphous phase, because voids are supposed to be generated in the amorphous phase during drawing [30]. The good fit of fibril dimensions to Equation 1 does not always indicate the spherulites to be uniaxially deformed. Equation 1 is also satisfied in the case of multi-directional drawing, if only the ratio of fibril cross-sectional area to that of spherulites is equal to the total draw ratio. In practice, the slender radial fibrils suggest the possibility of large stress towards the radial direction, because the observed value of fibril length is considerably greater than the value (9 μm) calculated in the same way as for radial fibrils. This stress may result from the centripetal component of necking stress, which drastically deforms spherulites and determines the morphology of the fibrils.

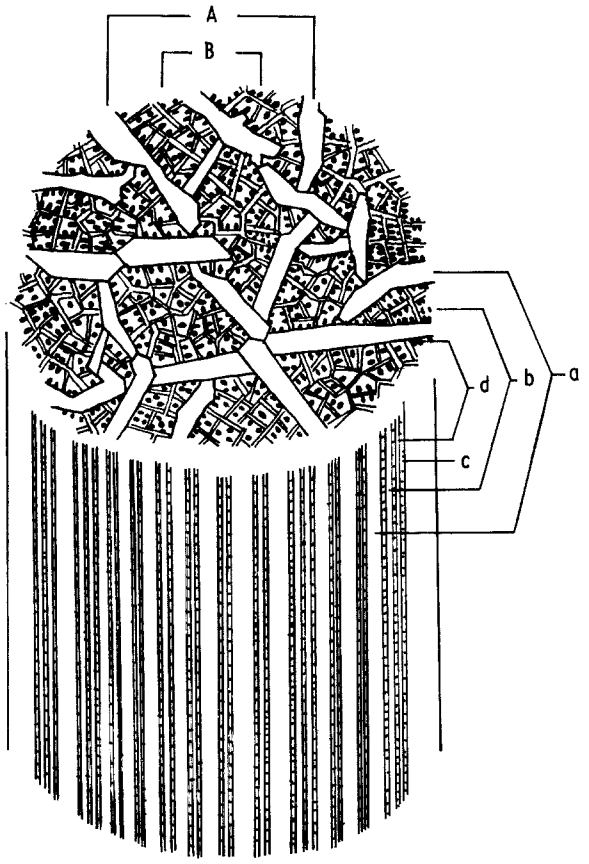

Figure 6 Schematic representation of the three-dimensional fibrillar structure of superdrawn POM fibres, showing the connection mode of the components of macrofibrillar structure including voids: A, frame network; B, sub-network; a, trunk fibril; b, branch fibril; c, cross-fibril; d, void.

4.2. Fibril model

The combination of the fibrillar structures of cross-section and longitudinal section produces an image of three-dimensional structure as shown in Fig. 6. In this picture, the fibrillar fibre consists of thick fibril screens parallel to the fibre direction which are bonded to frame fibrillar networks in the lateral direction, sub-networks in the frame cell, thin cross-fibrils connected to the networks and voids separated by cross-fibrils between the fibril screens. The model expresses the connection mode between aggregations of at least several tens of microfibrils at the submicrometre level: the trunk fibril continues to several hundreds of micrometres in length (corresponding to the unfolded spherulite length) to the fibre direction and is connected to other fibrils by interspherulitic components, and bridged to other fibrils to the lateral direction. The branch fibrils result from the breakdown of lamellar crystallites and have the same morphology as that of trunk fibrils, except for their thin thickness. Cross-fibrils and voids result from microfibrillation of the interlamellar phase at the fibril-shearing stage.

The frame network is very resistant to mechanical force due to the thick frame, crystalline continuity and crystallite bridging; on the other hand, the sub-network is fragile. The macrofibril model will be helpful in understanding the tensile strength, because the model gives several elemental parameters to assemble a fracture process, i.e. void size, fibril size and these quantities [31].

5. Conclusions

A fibrillar structure of superdrawn polyoxymethylene fibres was examined by scanning electron microscopy and the following points were elucidated.

1. The fibre has a skin–core structure. The skin layer is dense and the core layer consists of porous complex fibrillar networks. The morphology of the network in cross-section is characterized by a double network structure which consists of a frame network

of trunk fibrils, a sub-network of branch fibrils inside a cell constructing the frame, very thin cross-fibrils connecting to branching fibrils, and voids separated by cross-fibrils. Voids exist as a linear void-chain, like a ladder, between fibrils parallel to the fibre direction.

2. The relationships between the morphologies of the fibrils and the undrawn spherulites gave information on the origin of the fibrillar network and its components. The unit of the frame network originates in undrawn spherulites or small spherulitic crystallites in the region surrounded by spherulites. Trunk and branch fibrils result from a bundle of lamellar crystallites constituting spherulites. Crossfibrils probably result from the interlamellar amorphous phase.

3. The morphology of the fibrillar structure was heterogeneous in the radius direction: at the surface small square networks were formed, in the inside larger networks of radial fibrils were seen, and at the fibre centre, slender networks radially extending from the centre. The characteristic fibrillar structure is possibly related to the diversities of spherulitic morphology before drawing, and to the deformation stress acting on the spherulites during necking.

References

1. R. BONART and R. HOSEMANN, *Koll. Z.Z. Polym.* **186** (1962) 186.
2. N. KASAI and M. KAKUDO, *J. Polym. Sci.* **A2** (1964) 1955.
3. A. PETERLIN, *J. Polym. Sci.* **C9** (1965) 61.
4. M. TAKAYANAGI, K. IMADA and T. KAGIYAMA, *ibid.* **C15** (1966) 263.
5. A. PETERLIN, *Koll. Z.Z. Polym.* **216** (1967) 129.
6. *Idem, J. Mater. Sci.* **6** (1971) 490.
7. *Idem, Text. Res. J.* **42** (1972) 20.
8. D. C. PREVORSEC, P. J. HARGET, R. K. SHAMA and A. C. REIMSCHUESSEL, *J. Macromol. Sci. Phys.* **B8** (1973) 127.
9. A. PETERLIN, in "The Solid State Polymers", edited by P. H. Geil, E. Baer and Y. Wada (Marcel Dekker, New York, 1974) p. 83.
10. E. S. CLARK and L. S. SCOTT, *Polym. Engng Sci.* **14** (1974) 682.
11. A. G. GIBSON, G. R. DAVIES and I. M. WARD, *Polymer* **19** (1978) 683.
12. A. PETERLIN, in "Ultra-High Modulus Polymers", edited by A. Cifferi and I. M. Ward (Applied Science, London, 1979) p. 279.
13. A. J. PENNINGS and J. SMOOK, *J. Mater. Sci.* **19** (1984) 3443.
14. T. KONAKA, K. NAKAGAWA and S. YAMAKAWA, *Polymer* **26** (1985) 462.
15. A. E. ZACHARIADES and T. KANAMOTO, *J. Appl. Polym. Sci.* **35** (1988) 1265.
16. P. SMITH, P. J. LEMSTRA, J. P. L. PIJPERS and A. M. KIEL, *Coll. Polym. Sci.* **259** (1981) 1070.
17. M. IGUCHI, *Macromol. Chem.* **177** (1976) 549.
18. R. J. MORGAN, C. D. PRUNEDA and W. J. STEELE, *J. Polym. Sci. Polym. Phys. Ed.* **21** (1983) 1757.
19. H. MORISHITA, M. KOBAYASHI and T. KOMATSU, *Rep. Prog. Polym. Phys. Jpn* **30** (1987) 131.
20. W. HOOGSTEEN, H. KORMELINK and G. ESHUIS, G. ten BRINKE and A. J. PENNINGS, *J. Mater. Sci.* **23** (1988) 3467.
21. M. HOFF and Z. PELZBAUER, *Polymer* **32** (1991) 999.
22. T. KUNUGI, S. OOMORI and S. MIKAMI, *ibid.* **29** (1988) 814.
23. M. MATSUO and C. SAWATARI, *Macromolecules* **21** (1988) 1653.
24. M. MATSUO, C. SAWATARI and T. NAKANO, *Polym. J.* **18** (1986) 759.
25. A. O. BARANOV and E. V. PRUT, *J. Appl. Polym. Sci.* **44** (1992) 1557.
26. G. WU, K. TASHIRO, M. KOBAYASHI, T. KOMATSU and K. NAKAGAWA, *Macromolecules* **20** (1987) 2453.
27. K. TASHIRO, G. WU and M. KOBAYASHI, *Polymer* **29** (1988) 1768.
28. T. KOMATSU, S. ENOKI and A. AOSHIMA, *ibid.* **32** (1991) 1983.
29. *Idem, ibid*, **33** (1992) 2123.
30. J. H. WENDORFF, *Progr. Coll. Polym. Sci.* **66** (1979) 135.
31. T. KOMATSU, *J. Mater. Sci.* **28** (1993) 3035.

Received 15 May
and accepted 29 October 1992